Stereochemistry of Metalated Aldimines. 2. A Theoretical Study of Dimeric Ion-Pair Aggregates of Isomeric Lithioacetaldimines and of Their Kinetically Controlled Reaction with Formaldehyde

Rainer Glaser,*[1a,b] Christopher M. Hadad,[1a] Kenneth B. Wiberg,*[1a] and Andrew Streitwieser*[1c]

Departments of Chemistry, Yale University, New Haven, Connecticut 06511, University of Missouri, Columbia, Missouri 65211, and the University of California, Berkeley, California 94720

Received July 23, 1991

Our recent studies of isomeric monomeric metaloimine ion pairs showed a thermodynamic *anti* preference and the *syn* structures offered no explanation for a kinetic advantage. We thus proposed a mechanism involving dimeric ion-pair aggregates as the *reactive species* in order to account for the experimentally observed *syn* specificity in the reactions of metaloimines with electrophiles in solvents of low polarity. This hypothesis has now been tested at the ab initio level. Equilibrium geometries, vibrational frequencies, relative stabilities, and electronic structures of the C_i-symmetric dimers **3a** and **4a** formed by two *syn*- or *anti*-configured monomeric ion pairs of lithioacetaldimine, **1** and **2**, respectively, have been determined. The thermodynamic *anti* preference carries over from the monomers to the dimers; an *anti*-preference energy of 6.1 kcal/mol is found. The near perpendicular arrangement between the Li_2N_2 plane and the best plane(s) containing the anions emerges as an important structural concept and electrostatic interactions are likely as its electronic origin. Topologically related C_{2h} structures of **3** and **4** are disfavored. The analysis suggests and computations of the isomeric dimers formed by **1** or **2** with LiH, *syn*-**5** and *anti*-**6**, respectively, confirm that this mode of dimerization is maintained so long as at least one of the anions contains a (pseudo)-π-system. Potential energy surface scans of **5** and **6** show that distortions of the metal coordination that retain this structural feature require little energy while deviations from it require substantial energy. The activation energies required of **5** and **6** to meet distance requirements are discussed as well as ligand repulsion effects within the Li coordination sphere in the model system **7**, an H_2CO coordinated dimer formed by LiH and $LiNH_2$. Distance requirements alone cannot account for the kinetic advantage of the *syn* reaction, but the structures with optimal distance requirements suggest that precoordination and orientation of the reagent cause a kinetic advantage for the metal-assisted *syn* reaction as a result of ligand repulsion effects in the coordination sphere of lithium. As a concrete example, the transition-state structures **8** and **9** for the reactions of **5** and **6** with H_2CO have been determined. The Curtin–Hammett principle applies to the competition between the *syn* and the *anti* reactions and a preference of 0.9 kcal/mol for the transition-state structure of the *syn* reaction is found. These results suggest that the experimentally observed stereochemistry can be accounted for with a mechanism that involves a kinetically controlled reaction featuring *the dimer as the reactive species*. In contrast to metalated oxyimines, cooperative effects appear necessary to account for the stereochemistry of the additions of electrophiles to metaloimines under conditions that favor ion pairing and aggregation and the dimeric ion-pair aggregates appear as the smallest conceivable reactive species.

Introduction

Metalated N-substituted imines are important reactive intermediates for the regiospecific formation of a new CC bond in the α-position[3,4] to a carbonyl group without the disadvantages associated with the classical carbonyl chemistry.[5] One of the important characteristics of these metalorganic intermediates is the remarkably high specificity with which the *syn* products are formed,[6] that is, the products formed by the intermediate in which the N substituent and the CH_2 group are cis with regard to the CN bond. Accurate knowledge about the stereochemistry of the metalated intermediates is pertinent for discussions of reaction mechanisms, and many experimental studies have focused on the stereochemistry of these intermediates and their reactions with electrophiles.[7] In polar solvents,

Scheme I

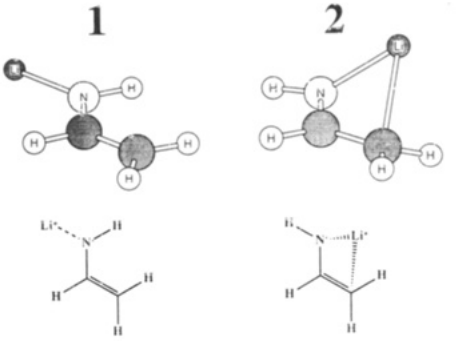

(1) (a) Yale University. (b) University of Missouri, Columbia. (c) University of California, Berkeley.

(2) For a discussion of the monomeric lithioacetaldimine, see: Glaser, R.; Streitwieser, A. *J. Org. Chem.*, previous paper in this issue.

(3) (a) Wittig, G.; Frommeld, H. D.; Suchanek, P. *Angew. Chem.* **1963**, *75*, 978. (b) Stork, G.; Dowd, S. R. *J. Am. Chem. Soc.* **1963**, *85*, 2178.

(4) Reviews: (a) Wittig, G.; Reiff, H. *Angew. Chem.* **1968**, *80*, 8. (b) Whitesell, J. K.; Whitesell, M. A. *Synthesis* **1983**, 517.

(5) (a) Stork, G. *Pure Appl. Chem.* **1975**, *43*, 553. (b) D'Angelo, J. Tetrahedron **1976**, *32*, 2979.

(6) (a) Thomas, J. *J. Organomet. Chem.* **1975**, *101*, 249. (b) Fraser, R. R.; Banville, J.; Dhawan, K. L. *J. Am. Chem. Soc.* **1978**, *100*, 7999. (c) Fraser, R. R.; Chuaquai-Offeremanns, N. *Can. J. Chem.* **1981**, *59*, 3007. (d) Fraser, R. R.; Banville, J. L. *J. Chem. Soc. Commun.* **1979**, 47. (e) Houk, K. N.; Strozier, R. W.; Rondan, N. G.; Fraser, R. R.; Chuaqui-Offermanns, N. *J. Am. Chem. Soc.* **1980**, *102*, 1426. (f) Fraser, R. R.; Chuaqui-Offermanns, N.; Houk, K. N.; Rondan, N. G. *J. Organomet. Chem.* **1981**, *206*, 131. (g) Fraser, R. R.; Bresse, M.; Chuaqui-Offermanns, N.; Houk, K. N.; Rondan, N. G. *Can. J. Chem.* **1983**, *61*, 2729. (h) Ferrman, H. E.; Roberts, R. D.; Jacob, J. N.; Spencer, T. A. *J. Chem. Soc. Commun.* **1978**, 49. (i) larcheveque, M.; Valette, G.; Cuvigny, T.; Normant, H. *Synthesis* **1975**, 256. (j) Cuvigny, T.; Larcheveque, Normant, H. *Tetrahedron Lett.* **1974**, *14*, 1237.

(7) (a) Ahlbrecht, H.; Deuber, E. O.; Enders, D.; Eichenauer, H.; Weuster, P. *Tetrahedron* **1978**, *39*, 3691. (b) Knorr, R.; Loew, P *J. Am. Chem. Soc.* **1980**, *102*, 3241. (c) Knorr, R.; Weiss, A.; Loew, P.; Raepple, E. *Chem. Ber.* **1980**, *113*, 2462. (d) Lee, J. Y.; Lynch, T. J.; Mao, D. T.; Bergbreiter, D. E.; Newcomb, M. *J. Am. Chem. Soc.* **1981**, *103*, 6215. (e) Meyers, A. I.; Williams, D. R.; White, S.; Erickson, G. W. *J. Am. Chem. Soc.* **1981**, *103*, 3088. (f) Meyers, A. I.; Williams, D. R.; Druelinger, M. *J. Am. Chem. Soc.* **1976**, *98*, 3032. (g) Meyers, A. I.; Poindexter, G. S.; Brich, Z. *J. Org. Chem.* **1978**, *43*, 892. (h) Meyers, A. I.; Williams, D. R. *J. Org. Chem.* **1978**, *43*, 3245. (i) Whitesell, J. K.; Whitesell, M. A. *J. Org. Chem.* **1976**, *42*, 377. (j) Horeau, A.; Mea-Jacheet, D. *Bull. Soc. Chim. Fr.* **1968**, 4571. (k) Kitamoto, M.; Hiroi, K.; Terashima, S.; Yamada, S. *Chem. Pharm. Bull.* **1974**, *22*, 459. (l) Fraser, R. R.; Akiyama, F.; Banville, J. *Tetrahedron Lett.* **1979**, *41*, 3929.

0022-3263/91/1956-6625$02.50/0

metalated imines most likely are dissociated into free ions and the reaction chemistry is determined by the thermodynamic *syn* preference of the isomeric anions. More typically, such reactions are carried out in solvents of low polarity and ion-pair formation and aggregation become important. Much of our work has therefore been directed at elucidating the structures, the relative stabilities, and the isomerization pathways of the possible ion pairs of metalated alkylimines,[2] metalated oxime ethers,[8] and dimetalated oximes.[9] We discussed monomeric ion pairs in these studies since the monomers generally are discussed in reaction mechanisms and because these monomers could still be the reactive species even if aggregation occurs in solution. For example, the lithioacetaldoxime ion pairs in the dimers retain their structural topologies and the assumption of reactive dimer shows no advantage.[10] In fact, the stereochemical preferences in the reactions of the metalated oxyimines all can be explained readily with the properties of the monomeric ion pairs.[11] In marked contrast, we have found that the structures and the isomer stabilities of the monomeric metaloacetaldimines are incompatible with the reaction stereochemistries observed. Our studies of the lithium ion pairs of acetaldimine have shown that the most stable *syn*-configured lithium ion pair, **1**, is planar and involves single N_σ coordination (**14** in ref 2) and that the most stable *anti* isomer, **2**, involves lithium π-coordination with a strong LiN contact and a relatively weak Li–C3 contact (**9** in ref 2), see Scheme I. The ion-pair formation reverses the relative isomer stability and an *anti*-preference energy of 5.32 kcal/mol[12] has been found for the ion pair. Primary solvation slightly reduces the *anti*-preference energy but the *anti* preference persists in the di- and trisolvated isomeric lithioacetaldimines.[2] These findings have led us to the hypothesis that dimeric aggregates—which are known to exist in solution[13,15]—might be the *reactive species* and an ion-pair catalysis mechanism for the kinetically controlled reaction toward the *syn* products has been proposed.[2]

Here the results are reported of an ab initio study of dimeric aggregates[16] of lithioacetaldimine and the reactions of model dimers with formaldehyde. To best approach the problem, one would wish to study the reactions of dimeric metalated N-alkylated imines with the inclusion of specific solvation. In theoretical ab initio studies, however, this approach meets with practical limitations and model systems need to be considered. We begin our study with a study of dimeric aggregates of ion pairs. Their analysis reveals characteristic properties, the structural concepts I and II, and we will then use model systems that reflect these properties. Even with the model systems, the computational task remains considerable and only the unsolvated systems were considered. These models reveal important information about the intrinsic differences of the reactions of the isomeric species that are pertinent to mechanistic discussions and that also are a prerequisite for future studies of systems that more closely resemble experiments. The equilibrium geometries and their vibrational frequencies and relative stabilities of the dimers **3a** and **4a** formed by combination of two *syn*- or two *anti*-configured monomeric ion pairs, respectively, have been determined and their electronic structures have been analyzed. Structural features are discussed in comparison to topologically related structures with different symmetry properties. The analysis suggests that the structural concepts found in **3a** and **4a** are typical for dimeric aggregates so long as one of the ion pairs contains a π-conjugated anion. Studies of the dimers formed between the isomeric lithioacetaldimines and LiH, *syn*-**5** and *anti*-**6**, support this structural concept, and these complexes are used to model the *syn* and *anti* reactions. Activation energies for distance requirements and ligand repulsion effects in the Li coordination sphere are examined with the model system **9**, a dimer formed between LiH and $LiNH_2$ and coordinated by H_2CO, to study the effects of metal assistance in the reaction. Proximity effects are found to be decisive in the reactions of the dimers and, as an example, the transition-state structures **8** and **9** for the reactions of the isomeric dimeric aggregates **5** and **6**, respectively, with formaldehyde are discussed.

Computational Methods

The structures of **3a** and **4a** were optimized at the levels RHF/3-21G[17] and RHF/3-21+G.[18] Vibrational frequencies were calculated analytically at the RHF/3-21+G level. More reliable energies were then computed with the 6-31+G* basis set[19] and with the 3-21+G structures, RHF/6-31+G*//RHF/3-21+G. As in the previous study[2] of the monomeric ion pairs, diffuse and d functions were omitted in the lithium AO basis set for reasons stated there. Other structures of **3** and **4** were examined and the potential energy surfaces of **5**, **6**, and **7** were scanned at the RHF/3-21G level. The transition-state structures **8** and **9** were first located with the minimal basis set STO-3G and then refined and characterized by analytical computation of the Hessian matrix at the RHF/3-21G level. Reliable relative energies of **8** and **9** were computed with these structures and with the 6-31+G* basis set, RHF/6-31+G*//RHF/3-21G. The RHF/6-31+G*/RHF/3-21+G wave functions of **3a** and **4a** and the RHF/6-31+G*//RHF/3-21G wave functions of **8** and **9** were analyzed topologically[20] with the program Extreme and integrated properties were determined on the basis of the theory of atoms in molecules[21,22] with the program Proaim. Ab initio calculations were performed with the Gaussian[23]

(8) (a) Glaser, R.; Streitwieser, A., Jr. *J. Am. Chem. Soc.* **1987**, *109*, 1258. (b) Glaser, R.; Streitwieser, A., Jr. *Pure Appl. Chem.*. **1988**, *60*, 195. (c) Glaser, R.; Streitwieser, A., Jr. *J. Am. Chem. Soc.* **1989**, *111*, 7340. (d) Glaser, R.; Streitwieser, A., Jr. *J. Am. Chem. Soc.* **1989**, *111*, 8799.

(9) Glaser, R.; Streitwieser, A., Jr. *J. Org. Chem.* **1989**, *54*, 5491.

(10) Glaser, R., Streitwieser, A., Jr. *J. Mol. Struct. (THEOCHEM.)* **1988**, *163*, 19.

(11) See the preceding three references.

(12) RHF/6-31+G*//RHF/3-21+G and including the zero-point energy corrections computed at RHF/3-21+G (ref 2).

(13) Gilchrist, J. H.; Harrison, A. T.; Fuller, D. J.; Collum, D. B. *J. Am. Chem. Soc.* **1990**, *112*, 4069.

(14) Metalated dialkylamides: (a) Galiano-Roth, A. S.; Collum, D. B. *J. Am. Chem. Soc.* **1989**, *111*, 6772. (b) Galiano-Roth, A. S.; Michaelides, E. M.; Collum, D. B. *J. Am. Chem. Soc.* **1988**, *110*, 2658.

(15) DePue, J. S.; Collum, D. B. *J. Am. Chem. Soc.* **1988**, *110*, 5518, 5524.

(16) Semiempirical MNDO calculations (Lee, K. H., Streitwieser, A., Jr., unpublished results) of the dimers formed by two *syn*- or two *anti*-configured monomeric ion pairs, respectively, suggested that these dimers are C_i-symmetric, but a good estimate of their relative stabilities could not be obtained at this level because of deficiencies of the semiempirical method (ref 10).

(17) 3-21G basis set: Binkley, J. S.; Pople, J. A.; Hehre, W. J. *J. Am. Chem. Soc.* **1980**, *102*, 939. Gordon, M. S.; Binkley, J. S.; Pople, J. A.; Pietro, W. J.; Hehre, W. J. *J. Am. Chem. Soc.* **1982**, *104*, 2197.

(18) Diffuse functions: Clark, T.; Chandrasehkar, J.; Spitznagel, G. W.; Schleyer, P. v. R. *J. Comput. Chem.* **1983**, *4*, 294.

(19) (a) 6-31G* basis set: Hehre, W. J.; Ditchfield, R.; Pople, J. A. *J. Am. Chem. Phys.* **1972**, *56*, 2257. Hariharan, P. C.; Pople, J. A. *Theoret. Chim. Acta* **1973**, *28*, 213. Binkley, J. S.; Gordon, M. S.; DeFress, D. J.; Pople, J. A. *J. Chem. Phys.* **1982**, *77*, 3654. (b) Six Cartesian second-order Gaussians were used for d shells.

(20) Extreme and Proaim: Biegler-König, F. W.; Bader, R. F. W.; Tang, T.-H. *J. Comput. Chem.* **1982**, *3*, 317.

(21) (a) Bader, R. F. W. *Acc. Chem. Res.* **1985**, *18*, 9. (b) Bader, R. F. W.; Nguyen-Dang, T. T.; Tal, T. *Rep. Prog. Phys.* **1981**, *44*, 893. (c) Bader, R. F. W. *Atoms in Molecules–A Quantum Theory*; Clarendon Press: Oxford, United Kingdom, 1990.

(22) (a) Bader, R. F. W.; Anderson, S. G.; Duke, A. J. *J. Am. Chem. Soc.* **1979**, *101*, 1389. (b) Bader, R. F. W.; Nguyen-Dang, T. T.; Tal, T. *J. Chem. Phys.* **1979**, *70*, 4316. (c) Bader, R. F. W. *J. Chem. Phys.* **1980**, *76*, 2871. (d) Bader, R. F. W.; Slee, T. S.; Cremer, D.; Kraka, E. *J. Am. Chem. Soc.* **1983**, *105*, 5061. (e) Cremer, D.; Kraka, E.; Slee, T. S.; Bader, R. F. W.; Lau, C. D. H.; Nguyen-Dang, T. T.; MacDougall, P. J. *J. Am. Chem. Soc.* **1983**, *105*, 5069. (f) Bader, R. F. W.; Essen, H. *J. Chem. Phys.* **1984**, *80*, 1943.

Table I. Structures of Dimers of Isomeric Lithioacetaldimine[a-c]

	syn dimer			*anti* dimer			
	3a		**3c**	**4a**		**4b**	**4e**
parameter	3-21G	3-21+G	3-21G	3-21G	3-21+G	3-21G	3-21G
N1–C2	1.4055	1.4033	1.3901	1.3814	1.3832	1.4001	1.3803
C2–C3	1.3291	1.3350	1.3294	1.3487	1.3512	1.3380	1.3432
N1–Li8	1.9262	1.9407	1.9047	1.9146	1.9242	1.9245	1.8865
N1–Li9	1.9264	1.9405	1.8864	1.9695	1.9970	1.9245	1.9437
C2–Li9				2.2807	2.3402	2.7202	2.4111
C3–Li9				2.4177	2.4667	3.0352	2.4277
Li8–Li9	2.2817	2.2842	2.0577	2.3246	2.3378	2.2942	2.0853
N1–N10	3.1042	3.1379	3.1841	3.1121	3.1490	3.0906	3.2132
N1–H4	1.0159	1.0152	1.0161	1.0074	1.0077	1.0077	1.0111
C2–H5	1.0805	1.0812	1.0901	1.0804	1.0806	1.0798	1.0792
C3–H6	1.0750	1.0761	1.0744	1.0769	1.0786	1.0776	1.0828
C3–H7	1.0717	1.0731	1.0713	1.0709	1.0720	1.0710	1.0698
N1–C2–C3	129.14	129.02	130.34	124.57	124.32	125.23	128.26
Li8–N1–C2	120.71	120.60	94.06	127.31	128.52	108.78	91.39
X–Li8–N1	53.69	53.95	56.70	54.33	54.85	90.00	
H4–N1–C2	109.39	109.93	107.88	111.91	112.13	111.45	108.99
H5–C2–N1	113.16	113.26	114.04	117.87	117.79	117.37	116.50
H6–C2–C1	121.87	121.99	121.58	121.69	121.94	122.30	125.67
H7–C2–C1	121.06	120.89	121.20	120.68	120.68	121.03	120.72
H4–N1–C2–C3	−0.01	0.02		180.15	181.13		
H5–C2–N1–H4	180.00	180.02		6.55	6.09		
H6–C3–C2–N1	−0.01	0.00		14.94	12.82		
H7–C3–C2–N1	180.02	180.00		184.89	184.24		
Li8–N1–C2–C3	136.41	136.87		−16.79	−18.45		
X–Li8–N1–C2	115.96	115.53		68.49	9.91		

[a] See Figures 1 and 2 for numbering. In angstroems and degrees. [b] **3a** and **4a** calculated in C_i symmetry. The symmetry of **3a** is de facto C_{2h}. **3c**, **4b**, and **4c** calculated in C_{2h}. [c] The label X symbolizes the inversion center.

series of programs on a Multiflow Trace7 computer and on various Vax workstations.

Results and Discussion

Dimeric Aggregates of Lithioacetaldimine. Structures. The dimers *syn*-**3a** and *anti*-**4a** result by dimerization of **1** or **2**, respectively. For reasons discussed below no dimers have been considered that are formed between ion pairs with different configurations. Structural parameters and the results of the vibrational analysis are summarized in Tables I and II, respectively. Energies and relative energies are listed in Table III. The optimizations at RHF/3-21G and RHF/3-21+G give similar geometries. Only the bond lengths involving lithium are slightly longer with the supplemented basis set (Table I). The structures obtained at RHF/3-21+G are discussed.

Geometry optimization of *syn*-**3a** within C_i symmetry results in the C_{2h} structure shown in Figure 1. The anions lie in a common plane and the lithiums are placed equidistant from each of the nitrogens in a perpendicular plane. The LiN bond lengths in the Li_2N_2 ring each are 1.941 Å, 0.163 Å longer than in the monomer **1**. The nitrogens are separated by 3.138 Å and the lithiums approach each other to a distance of 2.284 Å in bridging between the nitrogens.

The C_i-symmetric structure of *anti*-**4a** is depicted in Figure 2. The mode of metal coordination carries over from **2** to **4a**. Each Li coordinates in a π-fashion and, in addition, coordinates the N atom of the other anion. The bond lengths between Li9 and N1 and C3 are 1.997 and 2.467 Å, respectively. The corresponding distances in the monomer are 1.824 and 2.283 Å, respectively, that is, both of these distances are increased in **4a** by roughly 0.2 Å. The LiN distance of the additional metal nitrogen contact is 1.924 Å. Dimer **4a** might equally well be considered as a dimer formed by two η^1-N_σ-coordinated *anti* monomers (**10** in ref 2). Structural changes between those η^1 N_σ monomers and **4a** are rather small. The latter view would imply that the η^1 coordination mode is favored as more coordination sites are occupied.

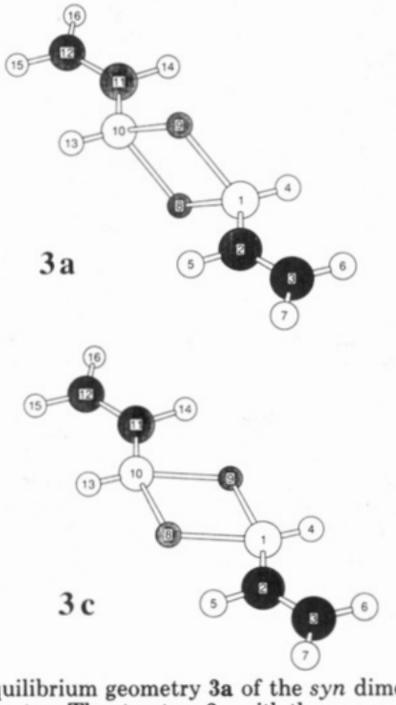

Figure 1. Equilibrium geometry **3a** of the *syn* dimer with de factor C_{2h} symmetry. The structure **3c**, with the same connectivity as **3a** but planar, is high in energy and unimportant.

The anion geometry in *syn*-**3a** is quite similar to that in **1**. The CN bond is sightly increased (by 0.017 Å) and the CC bond is marginally shortened (by 0.005 Å) on dimerization. Similar but slightly larger changes are found for *anti*-**4a**, where the CN bond is lengthened by 0.026 Å and the CC bond is shortened by 0.021 Å compared to **2**. These changes indicate that the electronic structures of

(23) Gaussian88 (Revision C) and Gaussian90 (Dev. Version, Release A), Frisch, M. J., Head-Gordon, M., Schlegel, H. B., Raghavachari, K., Binkley, J. S., Gonzales, C., Defrees, D. J., Fox, D. J., Whiteside, R. A., Seeger, R., Melius, C. F., Baker, J., Martin, R. L., Kahn, L. R., Stewart, J. J. P., Fluder, E. M., Topiol, S., Pople, J. A., Gaussian, Inc., Pittsburgh, PA, 1988.

Table II. Vibrational Frequencies of the Equilibrium Structures of the Isomeric Dimers of Lithioacetaldimine[a,b]

syn-**3a**		*anti*-**4a**	
ν	IRI	ν	IRI
33.5 u	9	66.6 u	3
55.9 u	1	94.2 u	4
91.8 g		134.7 g	
112.8 g		176.0 g	
144.5 u	2	201.3 u	12
224.6 g		259.1 g	
271.7 g		309.5 u	44
244.9 u	85	337.3 g	
463.4 u	155	422.3 u	112
499.1 u	133	496.4 g	
540.4 g		578.5 g	
554.0 g		583.6 u	48
633.9 g		611.2 g	
699.7 u	197	646.8 u	195
713.4 u	147	723.9 u	243
722.9 g		729.7 g	
833.4 g		782.5 g	
835.4 u	83	784.9 u	06
984.5 g		933.3 g	
986.2 u	428	945.2 u	479
1039.7 u	350	1061.5 g	
1043.4 g		1069.0 u	221
1157.2 g		1155.4 u	7
1157.7 u	31	1156.0 g	
1211.4 g		1233.7 u	35
1216.5 u	430	1239.4 g	
1462.0 u	97	1368.2 g	
1462.2 g		1388.2 u	621
1480.4 u	2	1465.3 g	
1480.4 g		1470.1 u	121
1604.9 g		1606.5 g	
1605.6 u	70	1607.7 u	7
1754.7 u	566	1742.5 u	376
1758.1 g		1745.1 g	
3246.8 g		3257.4 u	79
3247.1 u	85	3257.8 g	
3297.5 g		3285.0 g	
3297.6 u	12	3285.0 u	16
3380.2 g		3389.6 u	41
3380.3 u	55	3389.7 g	
3575.5 u	9	3671.7 u	198
3575.7 g		3672.2 g	

[a] Calculated at RHF/3-21G+G. [b] Frequencies in 1/cm and IR intensities in KM/mol.

Table III. Energies[a-c]

method	*syn*-**3a**	E_d	*anti*-**4a**	E_d	E_r
3-21G/3-21G	−278.426880		−278.433261		4.00
3-21+G/3-21+G	−278.454012	60.83	−278.461432	60.09	4.66
6-32+G*/3-21+G	−279.973167	57.09	−279.983246	52.90	6.32
VZPE(RHF/3-21+G)	80.31 (M)		80.53 (M)		

[a] Total energies in atomic units, vibrational zero-point energies (VZPE), and relative energies in kcal/mol. [b] VZPEs are not scaled. [c] Relative energy $E_r = E(syn) - E(anti)$. [d] Dimerization energy E_d with regard to **1** or **2**, respectively. E_d is defined as the negative of the reaction energy for the dimerization reaction. [e] Energies (RHF/3-21G) and relative energies (with regard to **3a** or **4a**, respectively) of **3c**, E = −278.377034 and E_r = 31.28, of **4b**, E = −278.428709 and E_r = 2.86, and of **4c**, E = −278.385718 and E_r = 29.83.

the anions become more imide like upon dimerization. Such an electronic reorganization would serve to increase the electrostatic interactions between the nitrogen and both of the lithiums, and, in the case of **4a**, to reduce the lithium contact with the CH_2 carbon, already relatively weak in **2**, even more.

Infrared Spectra. The vibrational frequency analysis shows **3a** and **4a** to be minima; there are no imaginary frequencies (Table II). As is typical for ion pairs, each of the dimers has several low-frequency modes that are associated with motions of the lithium cations. Small changes in some of the bond and dihedral angles involving lithium cation require little energy (vide infra). The vibrational frequencies of the dimers closely resemble those determined for the monomers at the same theoretical level.[2] As suggested also by the geometries, the monomeric ion pairs are altered comparatively little by dimerization.

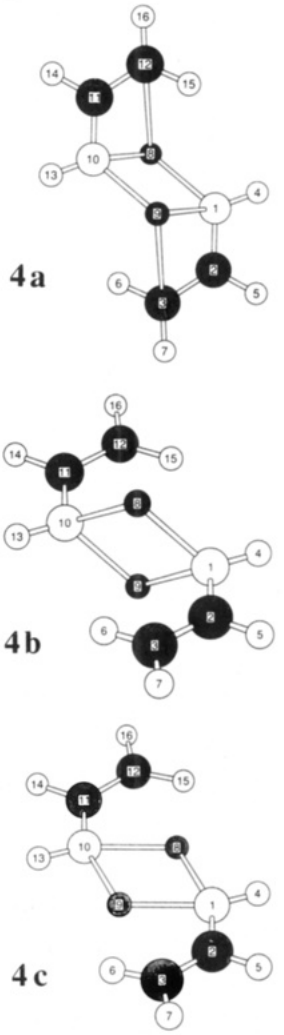

Figure 2. C_i symmetric structure **4a**, the equilibrium structure of the *anti* dimer **4**. The C_{2h}-symmetric structure **4b** is easily accessible from the equilibrium structure **4a**, while the planar structure **4c** is much less stable.

Energetics. The thermodynamic preference of the monomeric ion pair carries over to the dimers; *anti*-**4a** is more stable than *syn*-**3a** at all theoretical levels (Table III).[24] The *anti*-preference energy increases with the quality of the basis set, presumably because of the improved description of the cation-induced polarization of the vinyl groups in **4a**. At our highest level, RHF/6-31+G*//RHF/3-21+G, the *anti* preference is 6.32 kcal/mol and zero-point energy corrections[25] reduce this value slightly to 6.12 kcal/mol. While the *anti* preference prevails in the dimers, aggregate formation reduces the *anti* preference per ion pair by 2.26 kcal/mol to 3.06 kcal/mol.

(24) Basis set effects on dimerization energies for such reactions generally are small: (a) Hodoscek, M.; Solmajer, T. *J. Am. Chem. Soc.* **1984**, *106*, 1854. (b) Schleyer, P. v. R.; Pople, J. A. *Chem. Phys. Lett.* **1986**, *129*, 475. (c) See also: Sannigrahi et al. 1988, ref 32.

(25) Here and throughout this article the vibrational zero-point energy corrections are scaled (factor 0.9) to account for their unusual overestimation at this computational level.

The dimerization energies,[26] corrected for the vibrational zero-point energies, are 55.17 and 50.66 kcal/mol for the *syn*- and the *anti*-configured species, respectively. Aggregate formation is more exothermic for the *syn*-configured ion pair than for its isomer. Each of the monomeric ion pairs is stabilized by more than 25 kcal/mol upon dimerization in the gas phase. This stabilization is a few kcal/mol higher than the first solvation energy of lithium cation by typical ether molecules,[27] that is, ion-pair dimerization more than compensates for the loss of lithium solvation in ether solutions.

Electron Density Analysis of the Lithioacetaldimine Dimers. In topological electron density analysis[21] the molecular 3-dimensional electron density function $\rho(\mathbf{r})$ is characterized by its critical points, that is, points in Cartesian space where the gradient of the electron density is zero, grad $\rho(\mathbf{r}) = 0$. The critical points are classified depending on the signs of the principal curvatures λ_i of $\rho(\mathbf{r})$ by a pair of descriptors, the *rank* and the *signature*, where the *rank* specifies the number of non-zero eigenvalues of the second-derivative matrix of the density and the *signature* specifies the number of excess positive over negative principal curvatures. For the present discussion only two types of critical points are important, namely, (3,−1) bond critical points and (3,+1) ring critical points. The locations and pertinent characteristic values of the critical points of the electron density functions of **3a** and **4a** are summarized in Table IV. The partitioning of the electron density functions into spatial regions, the so-called basins, is defined by the zero-flux surfaces of $\rho(\mathbf{r})$, that is, surfaces for which the gradient of the density normal to the surface vanishes. The surfaces contain the bond and the ring critical points, and they define the spatial regions of the atoms in the molecules. Populations and kinetic energies of the atoms are derived by integration within the basins and, from the latter, the atom stabilities can be determined via $E = -T$ since the virial theorem ($V/T = -2$) holds for the quantum mechanical subspaces defined by this partitioning scheme. Atom populations and stabilities of **3a** and **4a** are summarized in Table V.

Electronic Structure of the Anions within the Dimers. Recently, we have shown that the anions of acetaldimine are best described as vinyl imides with vinyl groups that are strongly polarized in the fashion $CH(+)$-$CH_2(-)$.[28] The population data in Table V show that the presence of the lithiums reduces the anionic charge of the vinyl imides but little. Instead, the metal cation increases the N and reduces the CH_2 populations. Thus, *metal bonding is largely ionic and metal coordination in the dimeric ion-pair aggregates results in a more pronounced vinyl imide type electronic structure of the hydrocarbon fragments and reduces the polarity of the vinyl group.* For example,[29] in **3a** populations of 9.26, 6.58, and 8.07 electrons are found for the NH, CH, and CH_2 groups, respectively, while they are 8.95, 6.62, and 8.43, respectively, in the free *syn*-configured anion.[28,30] Metal coordination reduces the overall charge of $(CH_2{=}CHNH)^-$ by only 0.09 electron. The partitioning surface between C2 and C3 is moved little toward C3 in **3a** ($F_{C2C3} = 0.54$) compared to the free anion ($F_{C2C3} = 0.53$), whereas the CN bond critical point is significantly closer to C2 in **3a** ($F_{NC} = 0.63$) than in the anion ($F_{NC} = 0.58$). The CH population *increases* slightly despite these shifts of the partitioning surfaces primarily as a result of the stronger CC π-bond. The lower C bond polarity in **3a** compared to the free anion also is reflected in the $\rho(\mathbf{r})$ values at the CC bond critical points; $\rho(\mathbf{r})_{CC} = 0.35$ in **3a** and 0.29 in the anion. The vinyl imide type electronic structure further is manifested in the ellipticities of the CC and CN bonds of the dimers; large CC and small CN ϵ values are found.

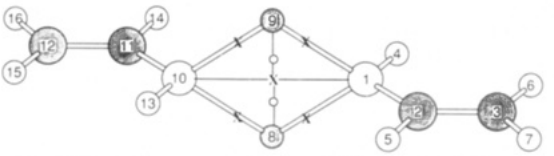

Figure 3. Schematic representation of the topological properties of the Li_2N_2 rings in **3a** (similar for **4a**). Bond critical points are marked "X" and ring critical points are marked by "O".

Topology of the Lithium Coordination in the Dimers. In Figure 3 the locations of the critical points are shown schematically that characterize the Li_2N_2 ring of **3a**. The molecular graph of **4a** is similar (except that two pairs of symmetry related LiN bond critical points occur while there are four such symmetry related critical points) and **3a** is discussed. Critical points of the type (3,−1) are marked by an X and (3,+1) ring critical points are marked by an O. Their characteristic parameters appear in Table IV. There is one (3,−1) critical point along each of the LiN bond paths. The scheme reflects the shape of these bond paths very well; the LiN bond paths actually are very well approximated by the straight lines shown. Interestingly, the inversion center is not a ring critical point. Instead, this point (no. 4) is a bond critical point with the eigenvectors of the Hessian matrix of $\rho(\mathbf{r})$ associated with the negative curvatures pointing perpendicular to the plane of the Li_2N_2 ring (λ_1) and toward the lithium atoms (λ_2), respectively. The eigenvector associated with the positive curvature traces out the NN bond path. The gradient paths originating at this critical point and following the directions defined by the eigenvector associated with λ_1 terminate at ring critical points (no. 5) as shown in Figure 3. The difference between the $\rho(\mathbf{r})$ values at the critical point no. 4 and at the ring critical points (no. 5) are *very* small; minor changes in the electron density function could cause these three critical points to coalesce to one single ring critical point. The proximity of the molecular graph of **3a** to a catastrophic point at which the molecular graph changes also is reflected in the extremely small value of λ_2, the curvature parallel to the Li–Li axis, and, as a consequence, by the large ellipticity of 1.626.

In molecular orbital theory the electronic structure of the isomeric vinyl imides and of the dimeric aggregates can be described equivalently in two ways depending on whether an sp^2- or an sp^3-type hybridization is invoked for nitrogen. The choice of either model is a matter of taste and merely changes semantics. In the N sp^2 model there would be one N_σ lone pair and one N_π orbital that would "conjugate" with the CC (pseudo)-π-system, whereas in the N sp^3 model there would be two equivalent N_σ lone pairs

(26) (a) The dimerization energies are the negative of the energies of reaction of the dimerization. (b) Energies (in atomic units) of the monomeric ion pairs at RHF/3-21+G and RHF/6-31+G*//RHF/3-21+G, respectively: *syn*-**1** 139.178539 and 139.941092 and *anti*-**2** 139.182839 and 139.949469. The vibrational zero-point energies (in kcal/mol as calculated at RHF/3-21+G) are 39.09 (**1**) and 39.02 (**2**). See ref 2 for details.

(27) Review: Karpfen, A.; Schuster, P. Ion-Molecule Interactions–A Quantum Mechanical Approach to Primary Solvation In The Chemical Physics of Solvation; Dogonadze, R. R., Kalman, E., Kornyshev, A. A., Ulstrip, J., Eds.: Elsevier; Amsterdam, The Netherlands, 1985.

(28) Glaser, R. J. *Comput. Chem.* **1989**, *10*, 118.

(29) Many attempts to integrate N and H(6) in *anti*-**4a** were unsuccesful due to the complicated zero-flux surfaces and because of small gradients. Since the structural effects associated with dimerization are the same for both isomers, it might be reasonable to assume that the electronic structures also are changed similarly.

(30) The analysis of the anions was carried out at RHF/3-21+G and small parts of these differences might thus be due to basis set dependencies.

Table IV. Bond Properties of the Isomeric Dimers 3a and 4a and of the Reaction Transition-State Structures 8 and 9

no.	A	B	r_A[b]	r_B	F[c]	ρ_b[d]	λ_1[e]	λ_2	λ_3	ϵ[f]
					syn-Lithioacetaldimine Dimer 3a					
1	N1	C2	0.885	0.518	0.631	0.309	−0.665	−0.641	0.162	0.038
2	C2	C3	0.727	0.609	0.544	0.352	−0.792	−0.535	0.166	0.480
3	N1	Li8	1.233	0.706	0.636	0.037	−0.064	−0.058	0.369	0.118
4	Li8	Li9	1.142	1.142	0.500	0.016	−0.012	−0.005	0.054	1.626
5	Li8	Li9	0.956	1.328	0.419	0.015	−0.013	0.011	0.051	
6	N1	H4	0.749	0.107	0.738	0.329	−1.157	−1.122	0.679	0.031
7	C2	H5	0.683	0.398	0.631	0.289	−0.785	−0.771	0.473	0.018
8	C3	H6	0.675	0.401	0.628	0.280	−0.743	−0.717	0.450	0.036
9	C3	H7	0.676	0.397	0.630	0.283	−0.760	−0.725	0.451	0.042
					anti-Lithioacetaldimine Dimer 4a					
1	N1	C2	0.878	0.507	0.634	0.323	−0.706	−0.670	0.164	0.054
2	C2	C3	0.732	0.619	0.542	0.344	−0.765	−0.531	0.186	0.440
3	N1	Li8	1.221	0.703	0.635	0.037	−0.065	−0.059	0.383	0.103
4	N1	Li9	1.268	0.732	0.634	0.029	−0.047	−0.043	0.294	0.100
5	Li8	Li9	1.169	1.168	0.500	0.015	−0.011	−0.005	0.052	1.280
6	Li8	Li9	0.955	1.383	0.408	0.015	−0.012	0.012	0.047	
7	N1	H4	0.749	0.259	0.743	0.336	−0.121	−0.118	0.718	0.029
8	C2	H5	0.691	0.390	0.639	0.290	−0.799	−0.792	0.484	0.008
9	C3	H6	0.675	0.403	0.626	0.277	−0.726	−0.692	0.049	0.049
10	C3	H7	0.677	0.395	0.632	0.283	−0.759	−0.724	0.450	0.049
					syn-Reaction Transition-State Structure 8					
1	N1	C2	0.886	0.456	0.660	0.347	−0.791	−0.763	0.480	0.037
2	C2	C3	0.742	0.626	0.542	0.334	−0.736	−0.542	0.207	0.358
3	N1	H4	0.753	0.263	0.741	0.331	−1.177	−1.154	0.697	0.020
4	C2	H5	0.688	0.392	0.637	0.293	−0.808	−0.802	0.484	0.007
5	C3	H6	0.676	0.400	0.628	0.280	−0.740	−0.705	0.447	0.051
6	C3	H7	0.675	0.399	0.629	0.282	−0.748	−0.710	0.446	0.054
7	N1	Li8	1.406	0.787	0.641	0.019	−0.027	−0.021	0.163	0.283
8	N1	Li9	1.197	0.694	0.633	0.039	−0.073	−0.065	0.425	0.124
9	Li8	H10	0.801	1.078	0.426	0.020	−0.026	−0.024	0.136	0.049
10	Li9	H10	0.771	1.003	0.435	0.025	−0.034	−0.032	0.177	0.040
11	Li8	Li9	0.947	1.499	0.387	0.012	−0.010	0.019	0.026	
12	Li8	O14	1.090	0.681	0.616	0.041	−0.084	−0.081	0.534	0.038
13	O14	C11	0.848	0.406	0.676	0.373	−1.014	−0.968	2.044	0.047
14	C11	H12	0.700	0.377	0.650	0.302	−0.868	−0.858	0.506	0.012
15	C11	H13	0.701	0.375	0.652	0.302	−0.872	−0.862	0.504	0.012
16	C11	C3	1.048	1.269	0.452	0.044	−0.042	−0.035	0.128	0.175
17	O14	N1	1.419	1.509	0.485	0.015	−0.011	−0.008	0.060	0.310
18	O14	N1	1.449	1.633	0.470	0.013	−0.010	0.010	0.058	
19	O14	N1	1.483	1.564	0.487	0.014	−0.013	0.020	0.046	
					anti-Reaction Transition-State Structure 9					
1	N1	C2	0.886	0.456	0.660	0.347	−0.791	−0.766	0.474	0.032
2	C2	C3	0.749	0.621	0.547	0.334	−0.737	−0.566	0.198	0.350
3	N1	H4	0.751	0.227	0.768	0.334	−1.193	−1.167	0.706	0.022
4	C2	H5	0.691	0.391	0.639	0.292	−0.803	−0.799	0.488	0.005
5	C3	H6	0.675	0.401	0.628	0.280	−0.740	−0.702	0.446	0.053
6	C3	H7	0.675	0.398	0.629	0.281	−0.748	−0.707	0.445	0.057
7	N1	Li8	1.376	0.774	0.640	0.021	−0.031	−0.025	0.188	0.208
8	N1	Li9	1.209	0.700	0.633	0.038	−0.068	−0.061	0.400	0.119
9	Li8	H10	0.805	1.094	0.424	0.019	−0.024	−0.023	0.130	0.047
10	Li9	H10	0.766	0.992	0.436	0.026	−0.035	−0.034	0.184	0.032
11	Li8	Li9	0.950	1.454	0.395	0.012	−0.009	0.019	0.025	
12	Li8	O14	0.679	1.083	0.385	0.041	−0.085	−0.080	0.542	0.059
13	O14	C11	0.849	0.407	0.676	0.373	−1.017	−0.961	1.972	0.058
14	C11	H12	0.699	0.378	0.649	0.301	−0.866	−0.854	0.507	0.013
15	C11	H13	0.701	0.376	0.651	0.301	−0.867	−0.857	0.505	0.012
16	C11	C3	1.017	1.236	0.452	0.049	−0.049	−0.041	0.139	0.196
17	O14	N1	1.547	1.456	0.515	0.013	−0.010	−0.005	0.053	1.036
18	O14	N1	1.484	1.625	0.477	0.011	−0.008	0.011	0.049	
19	O14	N1	1.480	1.570	0.485	0.013	−0.011	0.009	0.047	

[a] At RHF/6-31+G*//RHF/3-21+G for 3a and 4a and at RHF/6-31+G*//RHF/3-21G for 8 and 9. Compare Figures 3 and 8. [b] Distance r_A (r_B) of atom A (B) from the critical point in angstroms. [c] $F = r_A/(r_A + r_B)$. [d] Density at the critical point ρ_b (in e au^{-3}). [e] Eigenvalues λ_i of the Hessian matrix A of $\rho(\mathbf{r})$ at the critical point (in e au^{-5}). [f] $\lambda_n < \lambda_m$ and $\lambda_i < 0$ ($i = n, m$).

capable of "hyperconjugative" interactions with the vinyl group. In discussions of the interactions of cations with these anions it is important to realize that these models are interchangeable. For example, the latter model is more suggestive of covalent multicenter bonding contributions to the LiN bonding than the former model, and simply the choice of the model might lead to physically unwarranted conclusions regarding the bonding. One parameter, however, that can be used to investigate the LiN interactions is the molecular graph. In full support of the population data for Li and N, the LiN bond paths provide strong evidence against significant covalent contributions to LiN bonding. As pointed out above, these LiN bond paths virtually coincide with straight lines between the atoms, a feature typical for *ionic* bonding in small rings. Note also that all of the critical points in the LiN bonding region

Table V. Integrated Properties[a-d]

atom	N	T′	atom	N	T′
	syn-**3a**			*anti*-**4a**	
N	8.599	62.29252	N		
C2	5.551	37.56667	C2	5.507	37.48350
C3	6.058	37.78739	C3	6.182	37.76013
H4	0.661	0.47655	H4	0.639	0.46854
H5	1.027	0.63582	H5	0.992	0.62016
H6	1.012	0.61518	H6		
H7	1.001	0.61245	H7	0.990	0.60620
Li	2.091	0.39976	Li	2.089	7.36354
NH	9.260	62.76907	NH		
CH	6.578	38.20249	CH		
CH_2	8.071	39.01502	CH_2		
	syn-**8**			*anti*-**9**	
N	8.629	55.03080	N	8.634	55.03286
C2	5.294	37.43840	C2	5.302	37.43651
C3	6.126	37.84345	C3	6.115	37.84303
H4	0.647	0.47118	H4	0.643	0.47106
H5	1.001	0.63001	H5	0.995	0.62579
H6	1.005	0.61460	H6	1.008	0.61743
H7	1.003	0.61428	H7	1.000	0.61285
Li8	2.094	7.39279	Li8	2.093	7.39451
Li9	2.097	7.39028	Li9	2.097	7.39109
H10	1.890	37.05823	H10	1.891	0.64256
C11	4.869	37.05823	C11	4.857	37.05384
H12	0.963	0.62120	H12	0.968	0.62275
H13	0.953	0.61646	H13	0.957	0.61897
O14	9.437	75.52765	O14	9.443	75.52593
Σ	46.008	261.89082	Σ	46.003	261.88918
NH	9.276	55.50199	NH	9.277	55.50392
CH	6.295	38.06841	CH	9.277	38.06230
CH_2	8.134	39.07233	CH_2	8.123	39.07331
H_2CO	16.222	113.82353	H_2CO	16.225	113.82149

[a] At RHF/6-31+G*//RHF/3-21+G for **3a** and **4a** and at RHF/6-31+G*//RHF/3-21G for **8** and **9**. [b] Atomic populations N in electrons. [c] Integrated atomic kinetic energy corrected for the virial defect of the wave function, T', where $T' = T[-(V/T) - 1]$ and $-V/T$(*syn*-**3a**) = 2.00170614, $-V/T$(*anti*-**4a**) = 2.00172544, $-V/T$(**8**) = 2.00165062, and $-V/T$(**9**) = 2.00161441. [d] Properties of N in **3a** derived by difference.

are associated with rather small $\rho(\mathbf{r})$ values that are typical for ionic bonding. Multicenter bonding, which would have to involve Li p orbitals, would give rise to bond paths whose tangents at the Li locations would be nearly parallel to the plane(s) of the anions.

Mode of Dimerization. For the discussion of the reactivity of *syn*-**3a** it is significant that the plane containing the Li_2N_2 ring is *perpendicular* to the *common* plane of the anions. At the RHF/3-21G level the nonplanar C_{2h} geometry **3a** is preferred by 31.3 kcal/mol over the planar C_{2h} structure with the same connectivity, **3a** (Figure 1). The optimization of the electrostatic interactions between the Li^+ and the anions appears as a likely explanation for this preference. Only in the nonplanar structure are the Li cations placed in positions that allow for optimal electrostatic interaction with the π-density of the vinylimide anions.

In *anti*-**4a** the best planes of the anions remain perpendicular to the Li_2N_2 plane, to a first approximation, but the anions no longer share a common plane. The best planes that each contain one of the anions are separated by about 0.95 Å, and the parallel planes that contain the lithium cations lie approximately 0.47 Å away from these best planes. The loss of the common plane of the anions results from the additional $LiC(H_2)$ contacts. These contacts destroy the planarity of the anions and, thus, they remove the electronic feature that causes the C_{2h} symmetry in *syn*-**3a**.

The structure *anti*-**4b**, shown in Figure 2, was obtained at the RHF/3-21G level when C_{2h} symmetry was imposed. **4b** is only 2.9 kcal/mol less stable than the minimum **4a** at RHF/3-21G. This small energy difference clearly demonstrates that the $LiC(H_2)$ contacts are rather weak and that *distortions of* ***4a*** *along the reaction coordinate toward the* C_{2h} *structure* ***4b*** *require little energy*. The result that the Li_2N_2 plane is almost perpendicular to the best planes of the anions is a more significant structural concept. As with the *syn* dimer, changes in the dihedral angles between the Li_2N_2 plane and the planes of the anions require significant activation energy. The planar C_{2h}-symmetric structure **4c** is 29.8 kcal/mol less stable than **4a** at the RHF/3-21G level.

The preference for the structures **3a** and **4a** over the planar C_{2h} structures **3c** and **4c** has two important consequences. First, the discussion strongly suggests that a dimeric aggregate formed between one *syn*- and one *anti*-configured ion pair also would adopt a structure that is characterized by the four-membered Li_2N_2 ring and, more importantly, a structure in which this ring is approximately *perpendicular* to the (best) planes that contain the anions. Secondly, if the proposed explanation for the mode of dimerization is correct, then one would expect that this mode of dimerization also would carry over to dimers formed between different ion pairs *so long as at least one of these contains a* π*-system*. We will refer to these theorems as structural concepts I and II, respectively.

Thermodynamic versus Kinetic *syn*-Reaction Preference. The thermodynamic preference for the *anti* configuration carries over from the monomeric ion pairs to the dimers and its magnitude is only slightly smaller. A small thermodynamic *anti* preference persists even when the additional LiC contacts in the *anti* dimer are removed (as in **4c**). These findings suggest that the observed *syn* selectivity in reactions of metalated imines with electrophiles is not a consequence of a thermodynamic preference for the *syn*-configured reaction intermediate but rather is caused by kinetic control. Entry of the electrophilic reagent into the primary solvation shell of one of the metal cations could lead to a prereaction complex that could lower the energy of the reaction transition state for the bond formation at the α-C center and could increase the exothermicity of the reaction due to ion-pair formation in the products. Such a proximity effect might be responsible for a difference in the rates of reaction of the isomeric ion pair aggregates of metalated imines.

A qualitative consideration of the reaction with formaldehyde provides a rough estimate of the distance requirements for such proximity effects to become effective. With a carbonyl CO bond length of 1.2 Å, an LiO bond length of 2.0 Å (typical for O-solvated Li^+ ions[31]), an estimated CC bond length of about 2.0 Å in the reaction transition state, and assuming a 6-membered ring transition-state geometry with a chair conformation, one would expect an LiC_α distance of about 3.2 Å to be most suitable for optimal metal assistance in the reaction transition state.

In the minimum structure *syn*-**3a** the lithium cations are far removed from the reactive C center and distortions of the dimer structures are required if one of the metal cation should assist in promoting the reactions of electrophilic reagents with the dimer. In *anti*-**4a**, on the other hand, structural distortions would be required that increase the distance between one of the metal cations and the α-carbon. It is thus crucial to examine the energetic requirements of distortions of the dimers that place one of the cations in a more favorable position for proximity effects to become important. In the examination of these energetic requirements we make use of the structural

(31) Compare the above cited review by Karpfen et al., ref 27.

Table VI. Structures and Energies of the *syn* Dimers Formed with LiH[a,b]

parameter	5a	5b	5c	5d	5e
energy (−*E*)	147.18092	147.17968	147.17732	147.17493	147.17382
rel energy	0.00	0.78	2.26	3.76	4.46
N1–C2	1.4069	1.4091	1.4117	1.4111	1.4033
C2–C3	1.3289	1.3290	1.3298	1.3326	1.3386
N1–H4	1.0161	1.0152	1.0150	1.0147	1.0147
C2–H5	1.0803	1.0804	1.0798	1.0792	1.0784
C3–H6	1.0749	1.0752	1.0755	1.0760	1.0771
C3–H7	1.0717	1.0717	1.0719	1.0720	1.0720
N1–Li8	1.9143	1.8992	1.8894	1.8795	1.8732
N1–Li9	1.9143	1.9354	1.9482	1.9582	1.9933
C3–Li9	4.0654	3.8398	3.5744	3.1891	2.7695
H10–Li8	1.8256	1.8263	1.8276	1.8357	1.8418
H10–Li9	1.8256	1.8188	1.8158	1.8197	1.8271
Li8–Li9	2.3234	2.3133	2.3132	2.3352	2.3788
N1–C2–C3	129.00	129.00	128.87	128.48	127.73
H4–N1–C2	109.55	109.90	110.18	110.61	111.23
H5–C2–N1	113.17	113.25	113.41	113.79	114.34
H6–C3–C2	121.84	121.82	121.90	121.90	121.79
H7–C3–C2	121.09	121.09	121.01	120.97	120.94
Li8–N1–C2	120.28	122.81	125.31	127.00	125.90
Li9–N1–C2	120.33	112.65	104.86	93.08	82.27
H10–Li9–N1	103.11	102.93	102.59	101.59	99.63
H4–N1–C2–C3	0.01	11.60	20.70	27.57	33.06
H5–C2–N1–H4	180.01	189.36	196.92	202.47	205.37
H6–C3–C2–N1	0.01	−2.53	−4.36	−6.51	−10.13
H7–C3–C2–N1	179.98	179.35	178.94	178.41	177.18
Li8–N1–C2–C3	135.35	160.00*	180.00*	200.00*	220.00*
Li9–N1–C2–C3	−135.33	−114.70	−99.15	−86.58	−73.73
H10–Li9–N1–Li8	−0.66	0.20	0.43	0.85	0.45

[a] Calculated at RHF/321G in C_1. **5a** is de factor C_s. See Figure 4. [b] Energies in atomic units, bond lengths in angstroms, and angles in degrees. [c] Values marked by asterisks were kept fixed.

concept II, that is, we assume that the characteristic features of the dimers **3** and **4** carry over to the dimers **5** and **6**, respectively, formed by aggregation between LiH[32] and **1** and **2**, respectively. While scans of the potential energy surfaces of **3** and **4** are prohibitively computer time intensive, the model systems **5** and **6** are computationally significantly less demanding.

Distance Requirements for Metal-Assisted Reactions. Structural optimization of the dimeric aggregate formed between **1** and LiH at the RHF/3-21G level and without imposed symmetry constraints leads to the C_s-symmetric structure **5a** shown in Figure 4. As suggested by and in support of the above discussion, the plane of the Li_2N_2 ring[33] is perpendicular to the plane of the acetaldimine anion. For estimation of the energy requirement for distortions of **5** that allow for proximity effects, a scan of the potential energy hypersurface of **5** has been carried out. Four structures, **5b–e**, have been optimized with the dihedral angles Li8–N1–C2–C3 as the distortion coordinate with values in the range between 135° and 220°. This choice of the range of this dihedral angle places the Li8 atom within 45° of the equilibrium position of the lithium in the monomeric ion pair **1**. The structures thus obtained are shown in Figure 4 and structural parameters are listed in Table VI. With increasing values of the distortion coordinate the Li_2N_2 ring remains essentially perpendicular to the best plane of the anion. The imine H-atom is moved out of the NCC plane in the expected direction and assumes a dihedral angle of 33° in **5e**. Aside from this distortion and the relative position of the Li_2N_2 ring with regard to the anion, structural effects of the distortion are

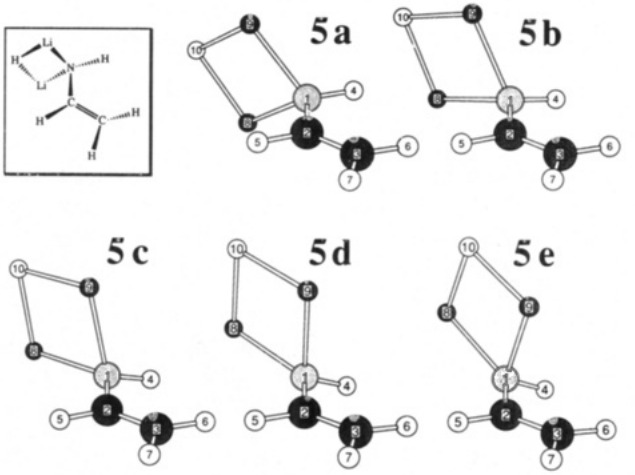

Figure 4. Geometries of the *syn* dimer **5**, formed by *syn*-lithioacetladimine and LiH, along the minimum energy pathway of the potential energy surface as a function of the (Li8–N1–C2–C3) dihedral angle. **5a** is the equilibrium structure.

generally small. As Li9 moves above the face of the anion, its π-type interaction with the vinyl group becomes more important as is clearly manifested in the typical distortions[34] of the anion, that is, the CH_2 group shows a tendency toward pyramidalization and it is slightly rotated around the CC axis toward Li9 and the H5 hydrogen is moved slightly out of the NCC plane toward the metal-coordinated face of the anion. Most importantly, the scan of the potential energy surface of **5** shows that *the energy requirement for distortions that place one of the cations in a favorable position for the promotion of reactions of the dimer with electrophiles is small.* The structure **5e**, the least stable structure among **5a–e**, is merely 4.5

(32) LiH is somewhat less polar than $LiNH_2$ but the bonding in LiH remains largely ionic: Sannigrahi, A. B., Kar, T. *J. Mol. Struct. (THEOCHEM.)* **1988**, *180*, 149.

(33) For discussions of LiX dimers, see, for example: (a) Kaufmann, E., Schleyer, P. v. R. *J. Comput. Chem.* **1989**, *10*, 437. (b) McKee, M. L. *J. Am. Chem. Soc.* **1985**, *107*, 7284.

(34) See refs 8a and 8b.

Table VII. Structures and Energies of the *anti* Dimers Formed with LiH[a,b]

parameter	6a	6b	6c	6d	6e
energy (−*E*)	147.18798	147.18309	147.18227	147.18105	147.18104
rel energy	0.07	0.00	0.51	1.28	1.29
N1–C2	1.3832	1.3848	1.3899	1.4042	1.4045
C2–C3	1.3475	1.3471	1.3450	1.3355	1.3352
N1–H4	1.0081	1.0079	1.0076	1.0088	1.0085
C2–H5	1.0800	1.0799	1.0796	1.0795	1.0796
C3–H6	1.0764	1.0767	1.0775	1.0772	1.0771
C3–H7	1.0708	1.0708	1.0707	1.0710	1.0710
N1–Li8	1.8953	1.8958	1.8971	1.9090	1.9108
N1–Li9	1.9843	1.9693	1.9350	1.9110	
C3–Li9	2.4183	2.4297	2.4931	3.0379	3.1101
H10–Li8	1.8041	1.8076	1.8166	1.8291	1.8303
H10–Li9	1.8394	1.8436	1.8565	1.8332	
Li8–Li9	2.3308	2.3367	2.3526	2.3253	2.3227
N1–C2–C3	124.39	124.38	124.46	125.21	125.26
H4–N1–C2	111.67	111.76	111.67	111.13	111.14
H5–C2–N1	117.79	117.77	117.67	117.16	117.09
H6–C3–C2	121.72	121.83	122.19	122.31	122.28
H7–C3–C2	120.69	120.70	120.68	120.99	121.02
Li8–N1–C2	129.19	127.70	124.30	114.50	111.44
Li9–N1–C2	81.92	83.49	88.73	108.41	
H10–Li9–N1	100.74	100.75	100.72	102.92	103.14
H4–N1–C2–C3	178.59	179.76	183.49	180.45	180.00
H5–C2–N1–H4	−7.60	−6.83	−3.57	−0.62	0.00
H6–C3–C2–N1	−14.77	−14.83	−14.18	−2.06	0.00
H7–C3–C2–N1	174.73	174.55	174.69	179.08	180.00
Li8–N1–C2–C3	10.00*	15.50	30.00*	40.00*	40.77
Li9–N1–C2–C3	−51.37	−48.97	−41.74	−41.48	−40.77
H10–Li9–N1–Li8	4.47	4.29	3.58	2.29	2.28

[a] Calculated at RHF/3-21G in C_1, except for **6e** (C_s). See Figure 5. [b] Energies in atomic units, bond lengths in angstroms, and angles in degrees. [c] Values marked by asterisks were kept fixed.

kcal/mol less stable than the minimum **5a**.

The energetic requirements of similar distortions in the model dimer **6**, formed between LiH and the *anti*-configured lithioacetaldimine **2**, have been examined by scanning the potential energy surface of **6** as a function of the dihedral angle Li8–N1–C2–C3 in the range between 10° and 40°. The results are listed in Table VII and molecular models are shown in Figure 5. Structure **6b** is the minimum with an *anti* preference of 1.4 kcal/mol with regard to the isomeric *syn* dimer **5a**. In **6b** the dihedral angle selected as distortion coordinate is 15.5°. A significant structural change occurs in the range between 30° and 40° of the distortion coordinate. In the structures **6a–c** the small pyramidalization of the C3 carbon remains relatively constant and the change in the distortion coordinate has little effect on the Li9–C3 distance. Once Li8 is forced sufficiently out of the NCC plane, then the Li9–C3 contact breaks, the C3 pyramidalization vanishes, and the anion becomes virtually planar. In **6d**, with a distortion coordinate of 40°, both of the lithiums are more than 3 Å away from the C3 atom. Optimization of **6** in C_s symmetry yields **6e**, a structure that is very similar to **6d**, and **6e** is likely to be the transition-state structure for racemization of **6b**. As with the *syn* dimer **5**, these distortions require little energy. Structure **6e** is only 1.3 kcal/mol less stable than the minimum **6b**. Note that this energy difference is just about half of the energy difference between the dimers **4a** and **4b**, that is, in both cases the loss of (one of) the Li–C3 contact(s) destabilizes the system by about 1.3–1.4 kcal/mol.

These calculations suggest that distance requirements alone do not result in a kinetic advantage for the reaction of the *syn* lithioacetaldimine dimer. On the contrary, the activation energy required for the *anti* dimer to place one of the lithium cations in a favorable position for reaction assistance is smaller than that for the *syn* dimer.[35] The

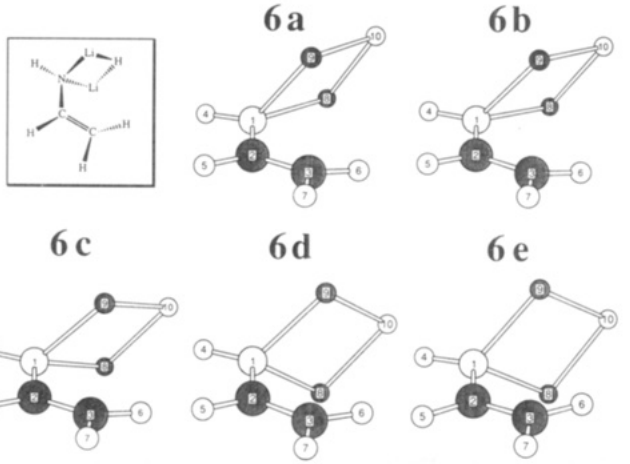

Figure 5. Geometries of the *anti* dimer **6**, formed by *anti*-lithioacetaldimine and LiH, along the minimum energy pathway of the potential energy surface as a function of the (Li8–N1–C2–C3) dihedral angle. **6b** is the minimum and C_s-**6e** is the transition-state structure for its enantiomerization.

model structures **6d** and **6e** would meet the distance requirement and only 1.3 kcal/mol of activation energy are required to reach this point on the potential energy surface. Among the *syn* structures, **5d** would be most suitable to promote a reaction and about 3.8 kcal/mol would be required for the distortion of the equilibrium structure **5a**.

Ligand Repulsion Effects. We have stated above that the Li and N atoms in the dimers **3a** and **4a** define a planar

(35) In using the activation energies of the model systems **5** and **6** as estimates for the activation energies of similar distortions in the dimers, we implicitly assume that the Li coordination of that anion of the dimer that does not undergo reaction remains relatively unchanged. In **4a**, for example, only the loss of one of the Li–C contacts is needed to meet the distance requirements for proximity effects.

Table VIII. Structures and Energies of the Model Complexes 7[a-c]

parameter	7a	7b	7c	7d	7e
energy (−E)	183.98712	183.98341	183.98568	183.97863	183.97588
rel energy	0.00	2.33	0.90	5.33	7.05
Li1–N	1.9374	1.9631	1.9342	1.9080	1.9322
N–Li3	1.8724	1.8667	1.8726	1.8815	1.8754
Li3–H4	1.7916	1.8183	1.7878	1.7317	1.8031
H4–Li1	1.9646	1.9054	1.9825	2.4654	2.0098
N–H5	1.0166	1.0165	1.0171	1.0173	1.0175
N–H6		1.0163	1.0163	1.0172	1.0152
Li1–O	1.8519	1.8780	1.8590	1.8427	1.9113
O–C	1.2127	1.2124	1.2130	1.2131	1.2115
C–H	1.0792	1.0793	1.0787	1.0789	1.0800
Li1–N–Li3	75.71	74.73	75.85	81.81	75.10
N–Li3–H4	108.29	107.56	108.33	118.57	107.45
Li3–H4–Li1	76.86	77.26	76.65	70.01	74.77
H4–Li1–N	99.13	100.43	98.61	89.61	107.46
H5–N–Li1	116.81	116.92	116.45	116.95	116.05
H6–N–Li1	119.77	121.25	117.30	117.03	118.83
N–Li1–O	138.45	110.00*	134.17	179.47	110.00*
H–C–O	116.52	121.78	121.71	121.57	121.83
H4–Li3–N–Li1	0.00	1.11	6.37	0.32	18.55
H5–N–Li1–Li2	116.44	116.45	113.96	116.27	109.42
H6–N–Li1–Li2	−117.77	−118.97	−116.47	−121.99	
Li3–N–Li1–O	180.00*	164.98	135.00*	90.00*	90.00*

[a] Calculated at RHF/3-21G in C_1, except for **7a** (C_s), with local C_{2v} symmetry for H_2CO and a linear N–Li–O arrangement. Other constrained parameters are marked by an asterisk. See Figure 6. [b] Energies in atomic units, bond lengths in angstroms, and angles in degrees. [c] See ref 36 for structures and energies of the isolated fragments LiH^*LiNH_2 and H_2CO.

4-membered ring that is (nearly) perpendicular to the (best) plane(s) of the anions. This typical feature—the structural concept I—also applies to all of the structures of **5** and **6**, and this feature might be crucial in the discussion of metal assistance in the reaction of the aggregates.

Consider the reaction of formaldehyde with the *syn* dimer **3a** or **5a**. Formaldehyde would enter the primary solvation shell of one of the lithium cations and a distortion of the dimer would have to occur such that the distance requirements for proximity effects are met, that is, a distortion of the type **5a** to **5d**. Formaldehyde could then easily assume a suitable orientation for the subsequent reaction with the α-C atom of the metalated imine. The imide N, the gegenion of the second ion pair in the dimer (another imide N in **3** or H in **5**), the reagent H_2CO, and perhaps an additional solvent molecule would coordinate to Li and the coordination sphere of this Li would be close to trigonal-planar or, when an additional solvent molecule is considered, pseudo-tetrahedral. Either way, the centers of negative charge of the dimer and the nucleophilic end of the reagent are relatively far apart. This situation is qualitatively distinct from the corresponding prereaction scenario in the *anti* dimers **4** or **6**. Structure **6d** meets the distance requirements and provides a good model. In order to orient H_2CO in a suitable position for reaction, the ligands around the lithium atom would have to assume a greatly distorted pseudotetrahedral arrangement in which the negatively charged atoms of the gegenions and the H_2CO oxygen are closer than in the corresponding scenario for the *syn* reaction. These qualitative considerations suggest that ligand repulsion terms might be responsible for the *syn* selectivity.

The model system **7**, a dimeric ion-pair aggregate[36] formed between LiH and $LiNH_2$ and with one H_2CO molecule coordinating to one lithium, was studied to estimate the magnitude of such ligand repulsion terms. Local C_{2v} symmetry of H_2CO and a linear Li–O–C arrangement were assumed for all structures of **7**.[37] Structure **7a** (Figure 6) was optimized under the constraint of C_s symmetry and all others were optimized in C_1 but with contraints on the H_2CO position. First we note that only small deviations from the planarity of the dimer $LiH{\cdot}LiNH_2$, imposed in **7a**, occur in **7b–e**, as can be seen from the respective dihedral angles in Table VIII. **7a** is the most stable structure among **7a–d**.[38] A small distortion of the (N–Li–O) angle in **7a** is all that would be

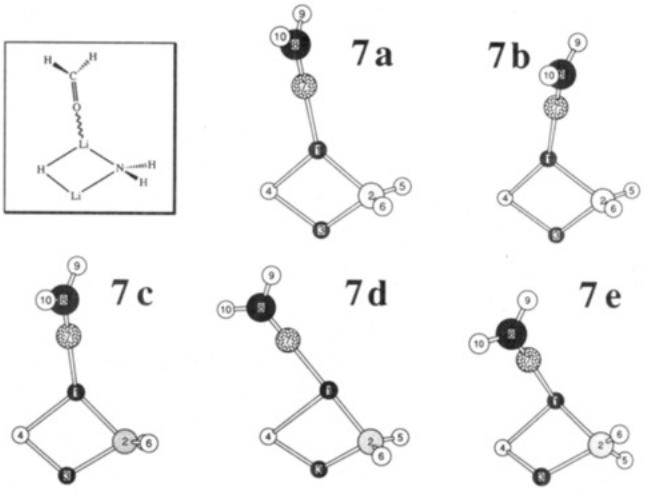

Figure 6. Structures of the model systems **7**.

(36) Structures and energies of the isolated fragments at RHF/3-21G. (a) LiH^*LiNH_2 in C_{2v}: n2–H4 = 2.9328, N2–Li1 = 1.8909, N–H = 1.016172, Li1–N2–H4 = 37.538, H5–N2–H4 = 126.974, E(RHF) = −70.730134. (b) H_2CO in C_{2v}: C–O = 1.2069, H–C–O = 122.528, C–H = 1.0833, E(RHF) = −113.22182.

(37) In **7**, the conformation of H_2CO with regard to the CO axis was chosen arbitrarily (H perpendicular to the (O–Li1–N) plane). This constraint has no consequences for the discussion.

(38) At RHF/3-21G **7a** is 22.1 kcal/mol more stable than the isolated molecules LiH^*LiNH_2 and H_2CO. While this value is likely to be overestimated due to the small basis set used, such basis set effects should have only small effects on the relative energies of the distorted structures of **7**.

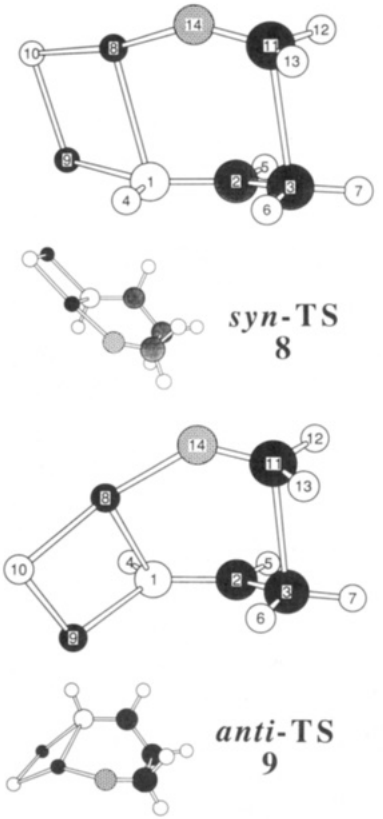

Figure 7. Reaction transition-state structures **8** and **9**, respectively, for CC bond formation in the addition of formaldehyde to the *syn* dimer **5** and the *anti* dimer **6**, respectively.

required to place the formaldehyde in a suitable position for the *syn* reaction. Optimization of **7** with a fixed (N–Li–O) angle of 110° results in **7b**. In this structure the H_2CO is moved slightly out of the best (2Li,N,H) plane and **7b** is 2.3 kcal/mol less stable than **7a**. Structure **7c** resulted when the dihedral angle between the (Li1,N,Li2) plane and the (O,Li1,N) plane was constrained to 135°, and **7c** is only about 1 kcal/mol less stable than **7a**. By constraining the same dihedral angle to 90° and with an appropriate initial structure we expected to obtain a suitable model for the ligand arrangement in the *anti* reaction, that is, a structure with a trigonal-pyramidal ligand arrangement in which the positions of one trigonal face are occupied. Instead, structure **7d** with de facto C_s symmetry resulted. Obviously it is energetically favorable to place the H_2CO oxygen and the imide N as far apart as possible, even if this requires a substantial elongation of the Li1–H4 bond distance. The Li1–H4 distance in **7d** is 2.465 Å, about 0.5 Å longer than that in **7a**, and this elongation is accompanied by a significant shortening of the Li1–N bond length. These features show a tendency of the dimer toward dissociation. A suitable model for the *anti* reaction, **7e**, was then obtained by imposing an additional constraint on the (O–Li1–N) angle, and this structure is about 7 kcal/mol less stable than **7a**.

Thus, the *syn* selectivity could be a kinetic phenomenon caused by ligand repulsion effects in the lithium coordination spheres of the dimeric ion-pair aggregates. The study of the simple model systems **7** indicates that such ligand repulsion effects could provide a kinetic advantage of about 5 kcal/mol for the prereaction scenario of the *syn* reaction. The magnitude of this effect probably is sufficient to overcompensate for the larger activation energy in the *syn* dimers associated with the distortions necessary to meet the distance requirements, and, thus, this ligand repulsion effect might be responsible for the overall kinetic

Table IX. Energies and Geometries of the Transition-State Structures 8 and 9 for the Addition of Formaldehyde to the Dimers 5 and 6, Respectively[a,b]

	syn-8		*anti*-9	
parameter	STO-3G	3-21G	STO-3G	3-21G
–*E*(STO-3G)	258.536303 (0.00)	260.431374 (0.00)	258.535923 (0.24)	260.429537 (1.15)
–*E*(3-21G)		260.442927 (0.00)		260.440489 (1.53)
–*E*(6-31+G*)		261.891012 (0.00)		261.889473 (0.97)
N1–C2	1.3913	1.3411	1.3940	1.3419
C2–C3	1.3535	1.3678	1.3524	1.3698
N1–H4	1.0315	1.0154	1.0301	1.0121
C2–H5	1.0898	1.0792	1.0943	1.0814
C3–H6	1.0786	1.0757	1.0780	1.0754
C3–H7	1.0773	1.0735	1.0775	1.0735
N1–Li8	1.9944	2.1925	1.9756	2.1496
N1–Li9	1.8215	1.8905	1.8371	1.9089
H10–Li8	1.7754	1.8779	1.7969	1.8978
H10–Li9	1.6600	1.7740	1.6415	1.7580
C3–C11	2.2537	2.3165	2.2128	2.2527
C11–H12	1.1006	1.0762	1.1034	1.0770
C11–H13	1.1027	1.0751	1.1014	1.0763
C11–O14	1.2491	1.2535	1.2499	1.2561
O14–Li8	1.6622	1.7693	1.6599	1.7618
N1–C2–C3	125.08	128.11	124.77	125.74
H4–N1–C2	106.79	111.33	106.73	111.60
H5–C2–N1	114.85	114.59	116.21	117.64
H6–C3–C2	119.98	119.93	119.73	119.66
H7–C3–C2	120.35	119.72	119.90	119.31
Li8–N1–C2	107.41	104.55	113.63	111.05
Li9–N1–C2	135.01	132.75	136.31	132.12
N1–Li8–H10	96.07	93.86	96.37	95.08
N1–Li9–H10	107.37	108.85	107.86	95.33
Li8–H10–Li9	83.06	84.05	81.38	81.77
C2–C3–C11	92.67	91.80	95.67	95.33
C3–C11–H12	90.46	89.34	95.93	93.46
C3–C11–H13	89.38	86.76	86.22	85.58
C3–C11–O14	108.00	109.78	106.78	108.57
C11–O14–Li8	140.40		138.31	133.87
H4–N1–C2–C3	–24.18	–13.56	173.74	172.75
H5–C2–N1–C3	192.06	188.30	189.49	186.40
H6–C3–C2–N1	19.27	17.54	20.48	17.01
H7–C3–C2–N1	177.33	175.10	177.00	172.60
Li8–N1–C2–C3	84.13	90.10	53.23	51.29
Li9–N1–C2–C3	167.54	170.47	–35.09	–33.15
H10–Li8–N1–Li9	3.78	1.90	–12.12	–9.47
C11–C3–C2–N1	–76.51	–79.37	–73.88	–79.23
H12–C11–C3–C2	–86.12	–86.10	–76.46	–75.68
H13–C11–C3–C2	159.19	158.91	–190.60	–189.98
O14–C11–C3–C2	37.12	37.08	48.23	48.61

[a] Total energies in atomic units, relative energies in kcal/mol (given in parenetheses), both lengths in angstroms, and angles in degrees. Calculated in C_1. See Figure 7. [b] Energies are based on the structures optimized at the level shown on top of the columns.

advantage of the *syn* reaction. It is emphasized that this kinetic advantage would be larger for the transition state of the *syn* reaction than for the prereaction model system **7**, because the negative charge is increased on the H_2CO oxygen in the (early) reaction transition state.

Transition-State Structures for the Addition of Formaldehyde to the Dimeric Ion-Pair Aggregates. As an example for the addition reaction of a carbonyl compound to a dimeric lithiated imine, the reaction transition-state structures **8** and **9** have been determined for the addition of H_2CO to the *syn*- and *anti*-configured model aggregates **5** and **6**. The structures of **8** and **9** were first determined with the minimal basis set and then reoptimized at the RHF/3-21G level. Structural parameters of **8** and **9** are listed in Table IX and the RHF/3-21G structures are shown in Figure 7. Vibrational frequencies were computed analytically at the RHF/3-21G level to confirm the stationarity of **8** and **9** and the vibrational frequencies together with their IR intensities are listed in Table X. **8** and **9** were also calculated at RHF/6-31+G*//RHF/3-21G to obtain wave functions for the topological electron density analysis and to obtain reliable

Table X. Vibrational Frequencies of the Reaction Transition-State Structures 8 and 9[a-c]

syn-8		*anti*-9	
ν	IRI	ν	IRI
−223.1	226	−261.4	340
130.5	7	104.6	8
140.7	20	122.4	21
178.4	21	166.7	14
226.7	4	213.7	14
275.6	58	303.3	57
318.6	16	338.5	13
353.9	6	387.5	47
435.3	145	429.9	194
459.1	314	454.0	290
514.8	158	575.5	52
651.3	12	608.5	68
682.1	110	671.4	44
785.2	7	811.4	16
844.6	22	823.4	51
866.0	180	843.0	82
899.7	332	873.7	563
972.7	706	945.6	609
1108.5	11	1117.2	31
1144.6	443	1173.9	307
1188.5	3	1185.5	93
1253.3	226	1248.3	208
1292.7	106	1284.5	53
1348.8	11	1346.8	10
1435.2	130	1427.5	167
1521.6	21	1504.4	92
1558.3	150	1551.1	273
1622.2	66	1622.6	5
1706.7	255	1739.4	123
1772.7	143	1773.1	151
3252.9	26	3238.8	31
3266.9	29	3242.5	45
3303.2	4	3303.5	2
3335.6	42	3319.2	50
3389.2	23	3390.3	23
3579.5	3	3611.1	1

[a] As calculated at RHF/3-21G. [b] Frequencies in 1/cm and IR intensities in KM/mol. [c] Vibrational zero-point energies are 65.47 (**8**) and 65.41 (**9**) kcal/mol.

relative energies. Results of the topological analysis and integrated properties are summarized in Tables IV and V, respectively.

Reaction Transition-State Structures. Both basis sets give transition-state structures with similar conformational characteristics. Each transition state contains a 6-membered ring formed by H_2CO, Li(8), and the heavy atoms of the imine anion. The 6-membered ring in **8** has an almost ideal chair conformation while the one in **9** is slightly twisted. Basis set dependencies show more significantly in the structural parameters: Lithium contacts always are shorter in the minimal basis set computations and comparatively long CN bonds result while the C(2)–C(3) bonds and the new CC bond are shorter. In the following only the 3-21G structures are discussed. The structural parameters of imine anions in **8** and **9** are rather similar to the respective values in the ion pairs. Only small changes of the CO bond lengths of H_2CO are found. The newly formed CC bonds are 2.32 Å (*syn*) and 2.25 Å (*anti*) long. As is typical for kinetically controlled reactions via early transition states (Hammond Postulate), the reaction transition-state structures closely resemble the reagents. This finding is fully consistent with the results of the electronic structure analysis.

Electronic Structures. The results of the topological analyses of the wave functions of **8** and **9** are summarized in Table IV. Somewhat unexpected is the occurrence of two ring critical points in the 6-membered rings (Li(8), H_2CO, and anion) of both transition-state structures. In

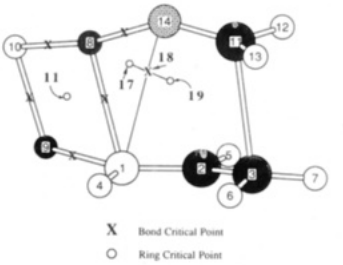

Figure 8. Schematic representation of the location of ring critical points in the *syn* reaction transition-state structure **8**.

Figure 8, the molecular graph is shown schematically for **8** (similar for **9**). Rather than the expected one ring critical point, there are two such points and a bond critical point in between. However, we consider this pecularity insignificant since the electron density in that region is low (less than 0.017) and its gradient is rather small.[39] The situation is similar to the one discussed above for the 4-membered rings in the dimers **3a** and **4a**. The 4-membered ring formed by the lithiums, the imide N, and the hydride H shows the molecular graph of a typical 4-membered ring in **8** and **9**.

The integrated charges reveal that only a quarter of the charge transfer from the imide anions to the H_2CO has occurred in the transition-state structures; the H_2CO charges are −0.26 (*syn*) and −0.23 (*anti*). Most of this electron density comes from the CH carbon since the lithiums keep charges in excess of +0.9 and because of the NH group charges are about the same in the dimer and in the transition-state structures. On the way to the transition states the imide anion essentially just increases the polarization of the CC π-density and loses some density from C(3) to H_2CO.

Relative and Activation Energies. With the minimal basis set a small preference of 0.24 kcal/mol is found for the transition-state structure **8** of the *syn* reaction. Single point calculations with these structures and with the 3-21G basis set resulted in a *syn*-reaction preference of 1.15 kcal/mol. Optimization of the reaction transition states at the RHF/3-21G level increased the preference for the *syn* reaction to 1.53 kcal/mol. Our best value for the relative energies of the reaction transition states was obtained at the RHF/6-31+G*//RHF/3-21G level: At this level a preference of 0.97 kcal/mol was determined for the *syn*-reaction transition structure. The (unscaled) vibrational zero-point energies of **8** and **9**, respectively, are 65.47 and 65.41 kcal/mol, respectively, and the inclusion of (scaled) vibrational zero-point energies thus reduces the relative energies by a marginal 0.05 kcal/mol to our final value $\Delta\Delta E_{act}$ = 0.92 kcal/mol for the relative energy of **8** and **9**.

The $\Delta\Delta E_{act}$ value for the difference in the activation energies for the *syn* and *anti* reactions offers a straightforward explanation for the observed *syn* selectivity of such reactions. The scenario is schematically[40] depicted in Scheme II. The *syn*/*anti* isomerization of the ion pair is fast even at low temperatures[2] and because of the Curtin–Hammett principle the product ratio will be de-

(39) Cf. Cioslowsky, J.; Mixon, S. T.; Edwards, W. D. *J. Am. Chem. Soc.* **1991**, *113*, 1083.

(40) In this study, we have considered only APE and $\Delta\Delta E_{act}$ and the actual activation energies have not been estimated. Note that the energies of the transition states are lower (25.2 for *syn* and 22.3 kcal/nol for *anti* at RHF/3-21G) than the combined energies of formaldehyde and **5** or **6** since **5** and **6** lack the lithium oxygen interaction associated with the precoordination. This interaction is on the order of 40 kcal/mol and it is significantly larger than the activation barrier for *syn*/*anti* isomerization of the ion pairs (ref 2).

Scheme II

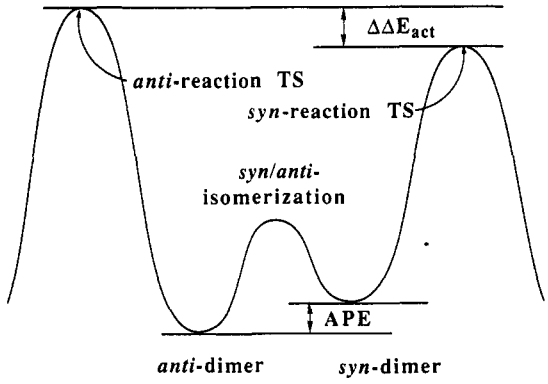

cided solely by $\Delta\Delta E_{act}$ and will not depend on the thermodynamic *anti* perference of the isomeric ion-pair dimers. Note that the value of $\Delta\Delta E_{act}$ is expected to increase for dimers such as **3** and **4** compared to the model systems **5** and **6**. That is, our results suggest that the *syn* selectivity is kinetically controlled and, moreover, that such dimers are the smallest conceivable reactive species that allow for an explanation of the experimentally observed stereochemistry at the molecular level.

Conclusion

The stabilization of each ion pair in the dimeric aggregates is significantly larger than are the heats of solvation of lithium cation with typical ethers, and ion-pair aggregation is therefore clearly implicated. The thermodynamic preference for the CN *anti*-configured lithioacetaldimine carries over from the monomeric ion pairs to the dimers. Our best estimate for the *anti*-preference energy is 6.1 kcal/mol. This theoretical result suggests that the *syn* selectivity of the reaction of the metalated imines is not determined by the relative thermodynamic stabilities of the dimeric intermediates but is the result of *a kinetic advantage of the syn reaction.*

While the relative isomer stabilities and the dimerization energies determine the abundance of the various metalated species in solution, they do not limit the array of a priori possible *reactive* intermediates. The activation energies to isomerizations are small and any species is thus readily available for reaction.[2] Any metalated intermediate, even if it were present in low concentration, might be the reactive species if its properties provide it with a kinetic advantage.[41] For example, ion-pair aggregation occurs in solutions of metalated oximes, metalated oxime ethers, and metalated hydrazones, but the aggregates formed show no apparent advantage for reaction and the monomeric ion pairs are likely to be the reactive species. In these systems the mode of metal coordination carries over from the monomers to the dimers and similar proximity effects would result for the reactions of the monomers as for dimers. This finding marks a fundamental difference between the metalated derivatives of N-heterosubstituted carbonyl derivatives and the metalated imines. In the case of the imines, the metal coordination mode is significantly affected by the dimerization and only in the dimers is the mode of coordination such that proximity effects might become operative. That is, in the mechanisms of the reactions of metalated imines in solvents of low polarity cooperative effects appear necessary to account for the *syn* selectivity of the reactions and *the discussed dimeric ion-pair aggregates appear as the smallest conceivable reactive species.*

The most stable isomeric dimers of lithioacetaldimine both are C_i symmetric. The near perpendicular arrangement between the Li_2N_2 plane and the best plane(s) containing the anions has been identified as an important structural concept and electrostatic interactions are likely as its electronic origin. The analysis suggests and computations of the model systems **5** and **6** confirm that this mode of dimerization is maintained so long as at least one of the anions contains a (pseudo)-π-system. The potential energy surface scans of **5** and **6** show that distortions of the metal coordination that maintain this structural concept require little activation energy, whereas planar structures (**3c** and **4c**) are high in energy and therefore unimportant. Distortions that allow for effective proximity effects in the metal-assisted reactions require small activation energies, but the activation energies are higher for the *syn* dimer than for the *anti* dimer and distance requirements alone cannot account for the kinetic advantage of the *syn* reaction. The structures with optimal distance requirements are such that the precoordination and orientation of the reagent would cause a significant advantage for the *syn* reaction as a result of ligand repulsion effects in the coordination sphere of lithium. Such effects are more pronounced in the reaction transition states and it is these effects that we consider responsible for the lower activation barrier of the reaction of formaldehyde with the *syn*-configured dimer. These results suggest that features of the coordination sphere of the gegenion are important for the understanding of these reaction mechanisms. Indeed, to fully appreciate the mechanism it is useful to regard the reactive intermediate as a ligand of the complexed gegenion. In general, this approach, the common approach in studies of *inorganic* mechanisms, might be beneficial also in related discussions of *organic* mechanisms.

Acknowledgment. This research was supported at UCB in part by NIH grant no. GM30369. C.M.H. graciously thanks the Fannie and John Hertz Foundation for a predoctoral fellowship.

(41) Note that in this work we have focused on an analysis of the differences of the reaction transition states for the α-C bond formation. Their relative energies are decisive if the activation barriers for these processes are higher than those associated with isomerizations (Curtin–Hammett). Studies of the transition states, of the prereaction complexes formed between the dimers and formaldehyde, and of pertinent isomerization barriers including specific solvation are in progress.